JOURNAL OF THE MECHANICAL BEHAVIOR OF BIOMEDICAL MATERIALS 55 (2015) 286–294

Available online at www.sciencedirect.com

ScienceDirect

www.elsevier.com/locate/jmbbm

Research Paper

Mechanical properties derived from phase separation in co-polymer hydrogels

R.M. Nixon[a], J.B. ten Hove[b], A. Orozco[c], Z.M. Jenkins[d], P.C. Baenen[a], M.K. Wiatt[e], J. Zuluaga[a], W.G. Sawyer[a,f], T.E. Angelini[a,g,h]

[a]Department of Mechanical and Aerospace Engineering, University of Florida, Gainesville, FL 32611, USA
[b]Laboratory of BioNanoTechnology, PO Box 8038, EK Wageningen, The Netherlands
[c]Department of Chemistry, University of Florida, Gainesville, FL 32611, USA
[d]Department of Physics, University of Florida, Gainesville, FL 32611, USA
[e]Department of Chemical Engineering, University of Florida, Gainesville, FL 32611, USA
[f]Department of Materials Science and Engineering, University of Florida, Gainesville, FL 32611, USA
[g]J. Crayton Pruitt Family Department of Biomedical Engineering, University of Florida, Gainesville, FL 32611, USA
[h]Instituite for Cell Engineering and Regenerative Medicine, University of Florida, Gainesville, FL 32611, USA

ARTICLE INFO

Article history:
Received 8 September 2015
Received in revised form
5 November 2015
Accepted 9 November 2015
Available online 18 November 2015

Keywords:
Hydrogel
Elasticity
Polymer
Phase separation
Failure strain

ABSTRACT

Hydrogels can be synthesized with most of the properties needed for biomaterials applications. Soft, wettable, and highly permeable gels with a practically unlimited breadth of chemical functionalities are routinely made in the laboratory. However, the ability to make highly elastic and durable hydrogels remains limited. Here we describe an approach to generate stretchy, durable hydrogels, employing a high polymer-to-crosslink ratio for extensibility, combined with an aggregating copolymer phase to provide stability against swelling. We find that the addition of aggregating co-polymer can produce a highly extensible gel that fails at 1000% strain, recovers from large strains within a few minutes, maintains its elasticity over repeated cycles of large amplitude strain, and exhibits significantly reduced swelling. We find that the gel's enhanced mechanical performance comes from a kinetically arrested structure that arises from a competition between the disparate polymerization rates of the two components and the aggregation rate of the unstable phase. These results represent an alternative strategy to generating the type of stretchy elastomer-like hydrogels needed for biomedical technologies.

1. Introduction

Soft, wettable, water-permeable materials are needed for biomedical technologies in which synthetic surfaces make intimate contact with delicate tissue cells and biopolymer networks (Holloway et al., 2011; Kubinová et al., 2011; Maki and Tambyah, 2001; Murakami et al., 1998; Šefca et al., 2002; Rongen et al., 2014; Spiller et al., 2011). Hydrogels possess these properties, and are easily synthesized with a wide range of biochemical functionality, but fall short in their material properties; hydrogels are notoriously brittle and lacking in durability (Baumberger et al., 2006; Naficy et al., 2011; Sachlos and Czernuszka, 2003; Tanaka et al., 2000). Hydrogel coatings of synovial joint prosthetics, for example, exhibit irrecoverable

http://dx.doi.org/10.1016/j.jmbbm.2015.11.003
1751-6161/

damage after just one cycle of sliding (Bavaresco et al., 2002). Many approaches have been taken to improve the material properties of hydrogels. Inspired by work on hard composites, hydrogels have been impregnated with nanoparticles to arrest crack propagation, though investigation of this failure mechanism in hydrogels continues (Gaharwar et al., 2011; Livne et al., 2005; Wang et al., 2012; Ye et al., 2014). Another approach has been developed in which a stretchy, elastic network interpenetrates a rigid, strong network (Gong et al., 2003; Jaramillo-Botero et al., 2010; Na et al., 2004; Yin et al., 2013). These gels have excellent strength and extensibility on par with many elastomers, though new approaches are being developed to increase their resilience; pioneering examples of double networks (DN) quickly lose their strength after only a few strain-cycles (Gong, 2010; Tanaka, 2007; Webber et al., 2007). Recovery of mechanical strength is achieved in very tough DN gels where ionic bonds are designed to break and reform, however their partial recovery requires added heat and occurs over hours or days (Sun et al., 2012). The development of a soft, elastomer-like hydrogel that can withstand large strains and recover within short periods of time would greatly broaden the applicability of hydrogels to many critical biomedical technologies.

Here we investigate a class of hydrogels inspired, in part, by the properties of elastomers. Stretchy elastomers attain their exceptional elasticity from a composition of long polymer chains at high concentration with very few crosslinks. In this manuscript we use the term *extensibility* to describe a material's strain at failure in extensional stress–strain testing. We synthesize polyacrylamide (pAAm) hydrogels at high concentration and low crosslink density, co-polymerizing with (hydroxyethyl)-methacrylate (HEMA). HEMA monomers can covalently bond to both acrylamide and to a shared crosslinker, bisacrylamide. To prevent swelling of the composite gel, we leverage the instability of polyHEMA (pHEMA), which aggregates at low concentrations. We explore the swelling kinetics, extensibility, and resilience of pAAm–pHEMA composite gels as a function of composition, finding that the addition of pHEMA to pAAm dramatically reduces swelling while maximizing hydrogel extensibility at a critical composition. We explore the physical origins of the composite gel's enhanced extensibility by characterizing the micro-structure, the nano-structure, and the polymerization kinetics of the co-polymer network. We find that small isolated nano-aggregates of pHEMA reduce network strength by interrupting the pAAm continuum, while extensibility is maximized when the polymerization rates of pHEMA and pAAm are matched and they form a bi-continuous structure. At this composition, the gel is highly extensible and resilient, recovering fully within four minutes after repeated cyclic strains up to about 400%, and failing at approximately 1000% strain. These results represent an alternative strategy to creating strethcy hydrogels, based on a balance between the extensibility of sparsely crosslinked hydrogels and the aggregating tendency of a phase separating co-polymer.

2. Materials and methods

2.1. Hydrogel synthesis

The gels studied here have a global polymer concentration of 27.2% (w/w), with varying relative amounts of (hydroxyethyl) methacrylate (HEMA) and acrylamide. Solutions of HEMA and acrylamide are gelled using 0.2% (w/w) ammonium persulfate, 0.2% (w/w) tetramethyl-ethylenediamine (TEMED), and 0.03% (w/w) N,N′-methylene-bisacrylamide crosslinker. Before polymerization, the solutions are gently pipette mixed, transferred into a mold made from PTFE tubing, and kept at 25 °C in a temperature controlled environment. All samples are 15 mm in length and 4.3 mm in diameter. Cured gels are removed from the tubing and stored in a humid environment at 25 °C. Tests are carried out 18 h after mixing and gels are tested in a humid environment to prevent drying.

2.2. Mechanical testing

We perform tension tests with a Malvern Kinexus rheometer. Cylindrical samples are secured to the tool and bottom plate with cyanoacrylate adhesive and encased in a humid environment while the rheometer extends the sample and records force and gap. This test provides failure strain and is used for resilience studies, where the sample is cycled through progressively larger strain amplitudes. Any failure data associated with detachment from the plates are discarded.

To characterize the kinetics of polymerization, rheological tests of elastic shear modulus are performed. The polymerizing mixtures are pipetted onto the rheometer configured with plate-plate geometry and a 1 mm gap. Immediately after pipette mixing and depositing the sample between the plates it is enclosed in a humid environment. Oscillatory shear strain tests are performed at a strain amplitude of 1% and an oscillation frequency of 1 Hz with the sample kept at 25 °C.

2.3. Structural characterization methods

Swelling measurements are performed on cylindrical samples submerged within a glass vial filled with ultrapure water. Changes in gel volume are monitored over the course of 40 h using time-lapse photography. Gel length and diameter are measured at each instant in time using Imagej software. Hydrogel microstructure is characterized by using time lapse microscopy at 90 × magnification on a Nikon inverted microscope. The sample is prepared by pipette mixing all of the components and wicking between two microscope coverslips with a 200 μm spacer. Samples are imaged with bright-field microscopy in transmission mode and with confocal microscopy using reflectance mode with a 488 nm laser.

2.4. Error and statistical analysis

Errorbars on extensional tests are standard deviations from repeated experiments on the same samples with the same composition. Errorbars on swelling tests are 95% confidence intervals from curve fits. A main effects analysis of variance (ANOVA) and a generalized linear model (GLM) were performed on the tension data to evaluate the significance of two factors: testing order, to determine if there was an evolution in the mechanical characteristics over time, and relative composition. Both the GLM and ANOVA give a p-value of essentially zero for the relative composition while giving 0.7 and 0.9, respectively, for the testing order. Therefore, the testing results did not significantly change with

successive tests but varied significantly with the relative composition. Additionally, post-hoc testing using Tukey's honest significant difference (HSD) shows the 66% composition is statistically different from every other composition tested.

3. Results

3.1. Composition and properties of hydrogel components

To leverage phase-separated aggregation in the stabilization of highly-elastic hydrogels with low crosslinking density, we co-polymerize acrylamide and HEMA at a global polymer concentration of 27.2% (w/w) and a bisacrylamide crosslinker concentration of 0.03% (w/w). Pure pAAm at this concentration and crosslinking density is expected to swell dramatically; a commonly used composition that does not swell after polymerization is 7.5% pAAm and 0.3% bisacrylamide. Here we decrease the crosslinker concentration by a factor of 10, and more than triple the monomer concentration. By contrast, pHEMA chains aggregate at 27.2%; optically clear, stable pHEMA hydrogels are typically formed at 65% pHEMA and 0.3% bisacrylamide. pHEMA gels with polymer concentrations below 60% are turbid due to chain aggregation (Gulsen and Chauhan, 2006; Nakamura, 1976). To investigate the balance of swelling and aggregation, and to study the structural and mechanical properties of these co-polymer hydrogels, we vary the relative concentration, ϕ, of pHEMA relative to pAAm from 0% to 100% (Fig. 1). Additionally, a range of formulations at different global polymer concentrations were explored (23–31%). An empirical search found that, within all of these formulations, a robust gel with great extensibility could be achieved. However, the whole grid of global polymer concentrations at the many different ratios of co-polymer was not explored, and even better formulations probably exist. The study presented here demonstrates the details of the over-all strategy, and leaves the door open for future studies to find the theoretical optimum for phase-separated gels.

3.2. Variation in hydrogel mechanics with composition

To test the potential effects of phase separated aggregates on hydrogel extensibility, we perform extensional stress–strain tests on cylindrical gel samples, prepared as described above. Samples are secured to the top and bottom plates in a rheometer using cyanoacrylate adhesive, and the gel is stretched by raising the upper plate at a rate of 0.1 mm s^{-1} while measuring the normal force. The extensional strain is given by $\gamma = \Delta L/L_0$, where ΔL is the extension length and $L_0 = 15$ mm is the initial sample length. Stress is given by F_n/A, where F_n is the measured normal force and $A = 14.5$ mm^2 is the cross sectional area of the samples. The failure strain is the highest strain before failure, or the strain corresponding to the point at which stress begins to drop rapidly to zero on the stress–strain curve. Pure pAAm gels fail at very large strains of around 1400%, and the addition of small amounts of pHEMA precipitously reduces the failure strain to a local minimum of 500% at a pHEMA concentration of 50%. With further increase of pHEMA to 66%, the failure strain rises again and peaks at 1000% strain. At concentrations above 66% pHEMA, the material weakens again and fails at lower strains, reaching a global minimum of 300% strain with the 100% pHEMA sample (Fig. 2a).

To relate the failure behavior of the gels to their linear elastic properties, we measure their moduli at low strains. The elastic moduli of the samples are determined by fitting lines to the first few percent of the extensional stress–strain curves and extracting slopes. The modulus of the two-component hydrogel varies non-monotonically with pAAm–pHEMA ratio, spanning a range of 10–120 kPa. This range of elastic modulus is comparable to the moduli of typical concentrated hydrogels and soft elastomers. The addition of pHEMA to pure pAAm reduces the modulus until 65–75% pHEMA is reached, and increases the modulus dramatically at higher pHEMA concentrations. We find that the softest two-component gels are also the most extensible. The non-monotonic dependence of modulus and failure strain on composition suggests that gels composed mostly of one component differ structurally from gels with comparable amounts of both polymers (Fig. 2b). An apparent discontinuity occurs between 50% and 66%, also suggesting that a structural phase change occurs across this boundary. Below, we explore this potentially

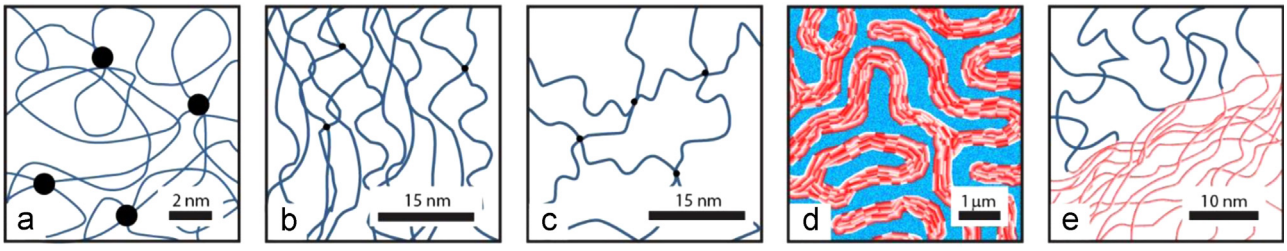

Fig. 1 – (a) A sparsely crosslinked network of concentrated pAAm yields an unstable, yet highly extensible gel. Scalebar: 2 nm. (b) Excess chain length relative to crosslink density results in high extensibility in unswelled gels (drawn slightly zoomed out to capture the crosslinks shown in (a)). Scalebar: 15 nm. (c) These sparsely crosslinked gels swell by about 600%, effectively pre-straining the network, reducing extensibility and increasing brittleness. Scalebar: 15 nm. (d) Phase separated aggregates of pHEMA (red) in pAAm (blue) background network. Unstable PHEMA interpenetrates and links to the pAAm network, forming a bi-continuous phase separated structure. Scalebar: 1 μm. (e) Close-up of phase boundary. Entanglements and labile bonds due to hydrophobic interactions form within the pHEMA aggregates. Scalebar: 10 nm. (For interpretation of the references to color in this figure legend, the reader is referred to the web version of this article.)

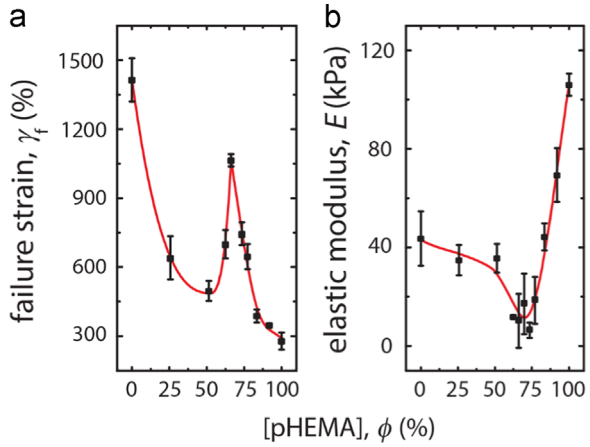

Fig. 2 – (a) Failure is shown as a function of relative pHEMA concentration in the 27.2% total polymer gel. Errorbars: standard deviation of repeated experiments. (b) The elastic modulus is found from the low strain linear region of the stress–strain tests. Errorbars: standard deviation of repeated experiments.

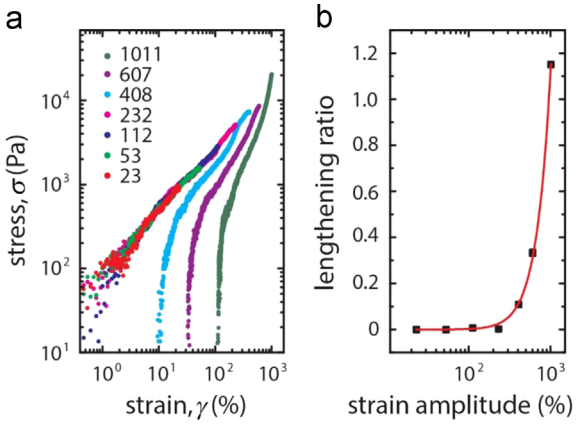

Fig. 3 – (a) Increasingly large strains are applied until failure occurs at over 1000% strain. Stress–strain curves begin to show fatigue at 408% strain amplitude. Legend: strain amplitude. (b) Relative change in the sample length at the start of each cycle, plotted vs the strain amplitude, shows the first sign of fatigue at 408%, where the gel has elongated by a factor of 0.1. A four minute delay time between cycles allows for the stretched gel to relax, though longer times may provide enhanced recovery.

sharp change in structure, which occurs when the pHEMA can form a system spanning structure that interpenetrates with a complementary system-spanning pAAm network.

To explore whether two-component gels possessing maximal elasticity are durable, we focus on the 66% pHEMA composition. We perform durability tests on this gel by cyclically stretching the gel with progressively larger strain amplitude, spanning 20–1000%. A delay of four minutes between tests provides time for the gel to recover to an unstrained state. The sequential stress–strain curves overlay very well up to a strain amplitude of about 400%, when the gel begins to lose elasticity at low strains. The loss of low strain elasticity does not immediately lead to failure; the gel stretches beyond 1000% in the final cycle before failing, which is the same as the strain achieved in single-pull tests. The onset of fatigue is observed in the lengthening of the gel; the gel first exhibits non-recovered elongation of about 10% at the beginning of the 400% strain cycle. Further studies must be carried out to identify the optimal recovery time; modest increases in recovery time may further reduce lengthening between tests and increase apparent durability (Fig. 3).

3.3. *Swelling reduction with the addition of aggregating polymer*

To investigate the potential effects of pHEMA aggregation on the swelling of pAAm, two-component gels are cast as cylinders of length $L=15$ mm and diameter $D=4.3$ mm. The hydrogel cylinders are removed from their molds, submerged in ultrapure water, and imaged in time-lapse for 40 h. The gels preserve their cylindrical shapes, so changes in length and diameter are used to compute volume changes over time. Traces in volume change over time are well fit by a saturating exponential curve, $V(t)=V_f(1-e^{-t/\tau})$, where V is the volume, V_f is the final equilibrium volume, t is time, and τ is a characteristic swelling time. By differentiating this curve, we determine an instantaneous swelling rate, $\dot{V}(t)=V_f\tau^{-1}e^{-t/\tau}$, or equivalently, $\dot{V}(t)=-\tau^{-1}(V-V_f)$, which also fits the swelling data (Fig. 4a,b).

We find that the pure pAAm gels swell by 600% over 40 h, consistently swelling at the highest rate with the largest time-constants. By contrast, gels with the highest pHEMA concentrations swell by about a factor of two at the slowest rates with the shortest time-constants. These results demonstrate that the addition of an aggregating co-polymer dramatically reduces bulk swelling. The data show a split in the swelling behavior around the 50% pHEMA composition, resulting in two distinct groups. The separation of swelling data into two groups suggests the existence of structural phase boundaries, which we explore below (Fig. 4c–d). These results, in combination with the mechanical tests above, show that the strategy taken here – enhanced extensibility through reduced crosslinking and swelling stabilization through phase-segregation and aggregation – produces durable, stretchy gels with rapid recovery times.

3.4. *Microstructural evolution of phase separated aggregates*

Visual inspection of the pAAm–pHEMA gels reveals a progression of structural heterogeneity across the different sample compositions. Pure pAAm gels are totally clear, while pure pHEMA gels are opaque and white in color. Between these two extremes, gels with small amounts of pHEMA become slightly turbid and translucent, while gels between 50% and 75% pHEMA appear opalescent, somewhat resembling the look of colloidal crystals. To investigate spatial heterogeneities within the gels at the microscale, pAAm–pHEMA mixtures are cast and cured between two microscope coverslips separated by 200 μm, and imaged with bright-field microscopy in transmission mode. To capture the temporal evolution of the structure, samples are imaged in time-lapse during curing.

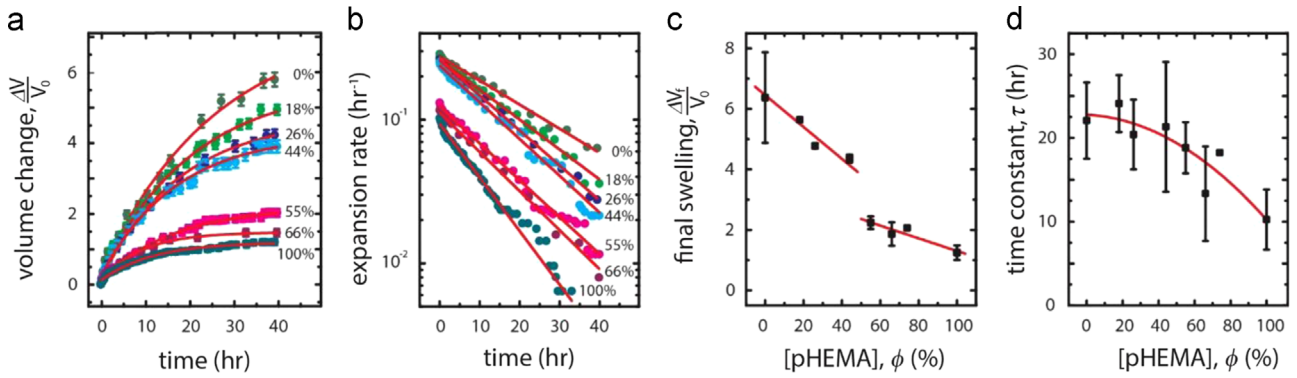

Fig. 4 – (a) Representative swelling curves showing relative percent volume change vs time. The compositions shown are the relative concentrations, ϕ, of pHEMA in the gel. Errorbars: standard deviations from repeated experiments. (b) The expansion rate is given as a function of time with the corresponding fits in red. (c) The final relative swelling is plotted as a function of the relative pHEMA composition showing a jump in swelling behavior. Errorbars: 95% confidence interval of fits. (d) The time constant, τ, is plotted as a function of composition, showing a reduction in the swelling time. Errorbars: 95% confidence interval of fits. (For interpretation of the references to color in this figure legend, the reader is referred to the web version of this article.)

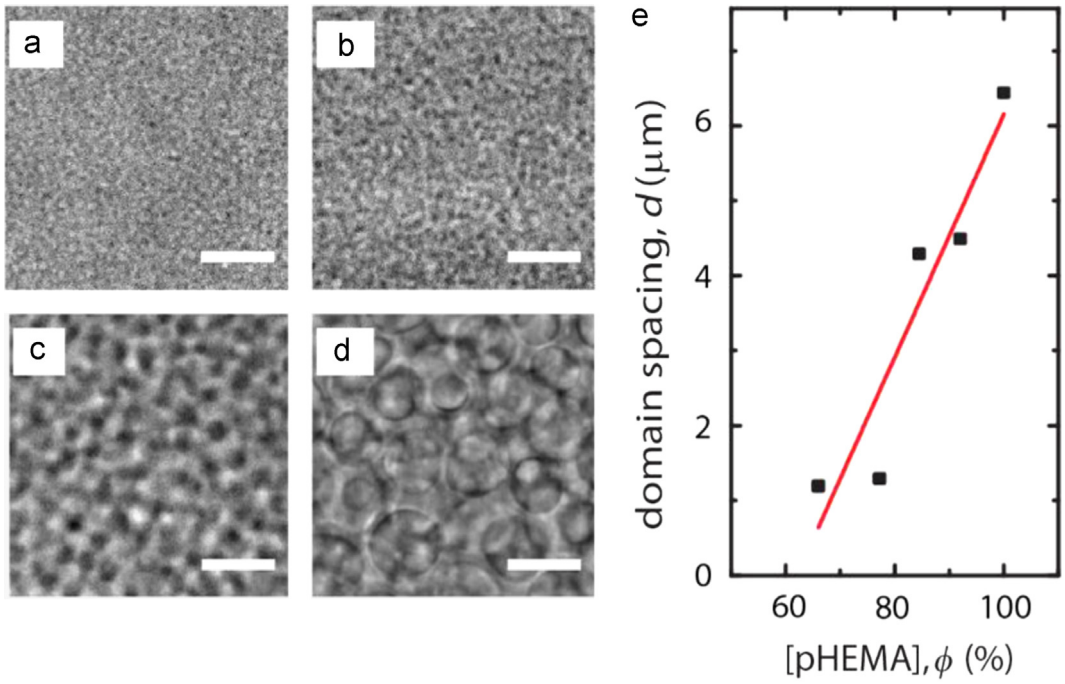

Fig. 5 – (a) The 66% pHEMA gel shows heterogeneities as small speckles with a 1 μm spacing. All scalebars: 6.5 μm. (b) 77% pHEMA shows a slightly coarser aggregate network (c) 92% pHEMA exhibits a greater characteristic spacing at nearly 4.5 μm. (d) 100% pHEMA has a large pore size, with an average spacing of 6.5 μm (e) Fourier analysis of micrographs gives domain spacing as a function of relative concentrations,ϕ, of pHEMA in the composite gel.

After curing is complete, 100% pHEMA gels exhibit large open pores that appear to be embedded within a continuous mesh, though 3D methods are required to determine the connectivity of these phases, described later. Fourier analysis of micrographs and direct measurements in real space show that the average spacing between pores is 6.5 μm. At lower pHEMA concentration with the addition of pAAm, the apparent pore size and spacing drop yet remains homogeneously distributed in space. At 66% pHEMA, the heterogeneities appear as small speckles with a characteristic spacing of 1 μm. Below 66%, no speckles are observed, though the samples attenuate and scatter the transmitted light (Fig. 5). The systematic trend in structure that evolves from pure pHEMA to 66% pHEMA suggests that at low pAAM concentrations the apparent continuous phase is pHEMA, and the pores are interconnected pockets of dilute pAAm gel. We have confirmed this with fluorescence imaging, where dissolved rhodamine exhibits higher intensity in the pore space, reflecting a reduction in solvent volume in the continuous phase.

Below 66%, no clear structural heterogeneities can be observed in the microscope with bright field illumination, so confocal reflectance microscopy is performed. Three dimensional stacks are collected in reflectance mode using a 488 nm laser. The aggregated structures generate a strong reflectance signal, enabling thresholding and cluster analysis to be performed. We filter noise from the images with a Gaussian kernel. The filtered stacks are thresholded by analyzing their voxel intensity histograms. Water or solvated polyacrylamide occupies most of the sample volume in all of the compositions explored here, so peaks in the histograms always occur at the low-end of the intensity range. The low-intensity peak in the histogram is used to threshold by assuming Gaussian-random statistics, choosing one standard deviation above the peak as the threshold. We set the low-intensity population equal to zero, and the high-intensity population equal to 1. The thresholded stacks are analyzed with 3D binary labeling code in MATLAB to determine the number and size of objects for each of the compositions.

We find small unconnected aggregates dispersed throughout the samples at low pHEMA concentration (26% relative polymer percentage, 7% absolute by volume). At this composition, the polyacrylamide appears to form a continuous solvated hydrogel that traps nano-scale pHEMA agglomerates. At intermediate pHEMA concentration (66% relative, 18% absolute by volume), the aggregated phase spans the entire system, with the two-component gel comprising two interpenetrating bi-continuous structures. We find that only about 2% of the volume is occupied by small-scale isolated aggregates. At the highest pHEMA concentrations (92% relative, 25% absolute by volume), the aggregated phase once again forms a continuous structure with micron-sized features and pore space as observed previously with bright field microscopy. Surprisingly, cluster analysis reveals that at all concentrations the non-aggregated solvated phase always spans the entire structure. Additionally at all concentrations, the volume fraction of aggregate is approximately equal to the total pHEMA concentration, indicating that the aggregated phase is composed of tightly packed HEMA chains (Fig. 6a–c). The same result is found from analysis of bright-field micrographs of pure pHEMA using bright field microscopy. The aggregated phase occupies an area fraction of 0.4, corresponding to an approximate volume fraction of 0.25, very close to the 27% global pHEMA concentration (Fig. 6d).

3.5. *Kinetics of two-component gel formation*

We perform curing tests in a rheometer to explore the potential role of disparate polymerization rates of the two monomer species in the ultimate structure and mechanical performance of the hydrogels. Immediately after the initiation of polymerization, the pAAm–pHEMA mixture is pipetted into a 1 mm gap between parallel plates and oscillated at 1 Hz with a 1% shear strain amplitude while measuring the elastic and viscous moduli, G' and G'', over time. We find that pure pAAm and pure pHEMA samples evolve rapidly, while pAAm–pHEMA mixtures take much longer to reach a saturating modulus value than either of the one-component gels. The curing curves for many two-component gels exhibit two shoulders, showing that multiple processes determine the steady-state hydrogel elasticity (Fig. 7a and c).

The mechanical curing tests on one-component gels reveal that acrylamide polymerizes at about twice the rate of HEMA. Interestingly, this difference in polymerization rate indicates that for compositions with less than 67% relative pHEMA, the pAAM component will complete the polymerization process first. Accordingly, $G'(t)$ and $G''(t)$ for the 66% pHEMA composition has a single-sigmoidal shape suggesting that both components cure at the same rate; at higher pHEMA concentrations, two features are observed in the curve (Fig. 7b and d) Thus, the consistent observation of physical transitions in gel properties near this boundary most likely arise from the differing polymerization kinetics of the two components and the resulting microstructure. The break-up of the pHEMA aggregates at relative concentrations below 66% suggest that the rapid gelation of pAAM arrests the phase separation process of pHEMA, trapping small aggregates into place, preventing pHEMA from forming system-spanning structures with a macroscopic shear modulus.

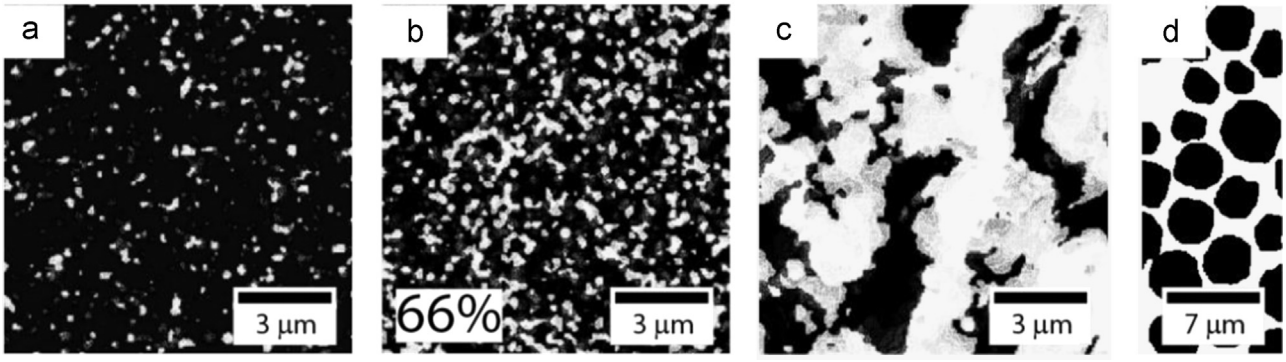

Fig. 6 – (a) Thin sections through 3D binary maps of aggregates are shown as shadowed surfaces, produced using volume viewer in Imagej. The 26% pHEMA (7% global) samples show small disconnected aggregates, occupying 9% of the total volume. (b) At 66% pHEMA (18% global) an interconnected morphology appears with the aggregating phase occupying 18% of the total volume. (c) 92% pHEMA (25% global) shows a larger scale connected aggregate occupying 27% of the total volume. (d) 100% pHEMA (27.2% global) is imaged with bright-field microscopy to reveals an area fraction occupied by the aggregated phase of 0.4, corresponding to a volume fraction of about 25%.

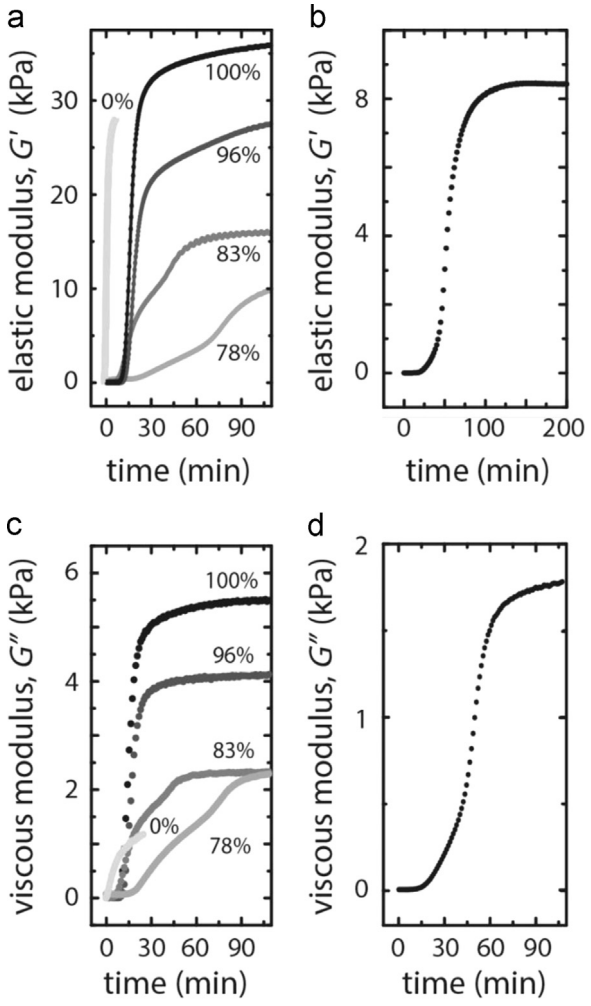

Fig. 7 – (a) Elastic shear modulus plotted as a function of time during the cure demonstrates disparate polymerization kinetics of different components and variation with mixtures. Pure pAAm and pure pHEMA cure rapidly. Mixtures of the two polymers have increased equilibration times. Curves are labeled with the relative amount of pHEMA in the corresponding sample. (b) The shear modulus as a function of time during gelation of the 66% pHEMA evolves as a single-sigmoidal indicating that both components polymerize at the same rate at this composition. (c) The viscous shear modulus, G″, is much smaller in magnitude than G′ throughout the curing process, showing that the response of the system is dominated by its elastic component. (d) The viscous modulus of the 66% pHEMA sample shows a single equilibration time-scale.

4. Discussion and conclusions

The strategy described here for enhancing hydrogel extensibility and durability leverages a well-known behavior of polymer networks: decreased crosslinking density increases extensibility, while increased crosslinking density increases brittleness. The compromise that comes with reducing crosslinking density is the tendency of under-crosslinked networks to swell. This potential drawback is mitigated by co-polymerizing an unstable component into the network that aggregates, driving the network to contract against swelling forces. We have found that with this approach comes a rich breadth of phenomena that couple the kinetics of polymerization and aggregation with microscale and nanoscale structure. The stable component of the copolymer gel, pAAm, polymerizes much faster than the aggregating component, pHEMA, rapidly generating a system-spanning network that inhibits pHEMA aggregation as it slowly polymerizes, controlling the spatial distribution of phase separated structures. The resulting gel has widely tuneable mechanical properties, and can be designed to achieve a targeted balance of elasticity and stability against swelling.

The pioneering examples of the double network (DN) approach to hydrogel synthesis have provided tremendous enhancement of gel strength and elasticity (Chen et al., 2012). The more recent efforts to enhance durability build on the DN concept by building in labile bonds – links that can be broken and re-formed (Kong et al., 2003; Sun et al., 2012). The early DN networks and the more recent DN networks with labile bonds are both based on structures that interpenetrate at the scale of the network mesh-size – about 10 nm or less. Illustrations of these networks found in the literature show the double networks and bond forming polymers crossing one another over these extremely short lengthscales. The phase-separation and aggregation approach taken here also represents a form of labile bond formation. Precipitated agglomerates of pHEMA chains can be pulled apart since branching is minimized by maintaining a low crosslinking density relative to chain length. The network elasticity and the driving force to re-form these non-specific hydrophobic bonds is provided by the highly stretchable pAAm network; gels with very little pAAm break at very low strain levels. In these gels, the labile bonds are grouped in larger phase-segregated structures that are most effective when the spatial scale of separated domains is about 1 μm. We hypothesize that the rapid recovery of these gels after large strains can be attributed to this large spatial scale; individual dangling bonds do not have to find one another and re-connect. Rather, if the large-scale "bonding network" of aggregated pHEMA does not break up under stretch, then spatial pathways to structural recovery facilitate the rapid relaxation of strain when applied stress is released (Fig. 8). Future studies will uncover the structural evolution of phase separated domains during stretch and recovery, enabling the development of more extensible and durable hydrogel materials.

For load bearing biomedical implants, the hydrogel created here would be limited to applications in which maximum stress levels remain below about 10 kPa. Interestingly, micro-phase separation in biopolymer systems of proteins and polysaccharides frequently occurs (Capron et al., 2001). In these systems, living cells could be incorporated into one or both phases during the gelation process. Thus, our approach to creating stretchy, robust gels could be used in contexts where cell encapsulation is desired for therapeutic or biosensing applications.

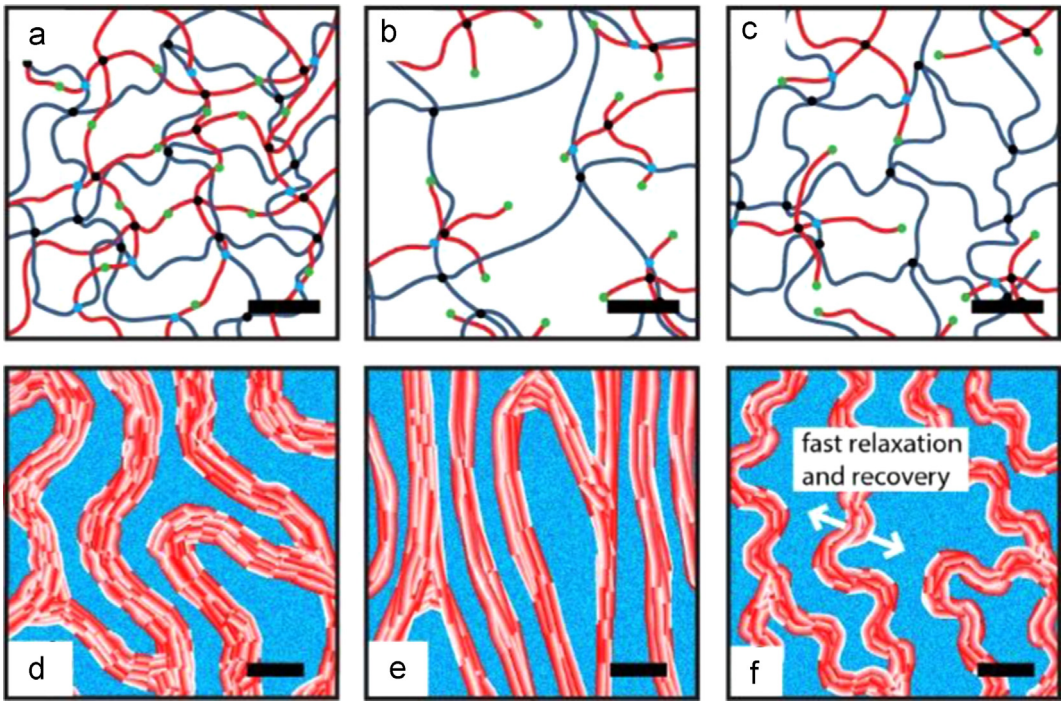

Fig. 8 – (a) Recent developments in double network (DN) gels utilize an interpenetrating network capable of labile bonding. Scalebar:10 nm (b) when stretched these networks break their labile bonds, dissipating energy while preserving a more extensible secondary network. Scalebar: 10 nm (c) after the material is unloaded it takes a great deal of time and even the addition of heat to recover individual dangling bonds into a re-configured DN after a large strain. Scalebar: 10 nm (d) a phase-separated microstructure consisting of two interpenetrating bi-continuous structures: a highly extensible background network and a stabilizing aggregated phase. Scalebar: 1 μm (e) the aggregated phase forms non-specific hydrophobic labile bonds that can be pulled apart as the gel is extended while maintaining a network pathway throughout the background network. Scalebar: 1 μm (f) the aggregated phase rapidly reforms non-specific labile bonds when the network is unloaded and spatial pathways preserved by the background network provide means for rapid relaxation and recovery. Scalebar: 1 μm.

REFERENCES

Baumberger, T., Caroli, C., Martina, D., 2006. Solvent control of crack dynamics in a reversible hydrogel. Nat. Mater. 5, 552–555, http://dx.doi.org/10.1038/nmat1666.

Bavaresco, V.P., Zavaglia, C.A.C., Malmonge, S.M., Reis, M.C., 2002. Viability of pHEMA hydrogels as coating in human synovial joint prosthesis. Mater. Res. 5, 481–484.

Capron, I., Costeux, S., Djabourov, M., 2001. Water in water emulsions: phase separation and rheology of biopolymer solutions. Rheol. Acta 40, 441–456, http://dx.doi.org/10.1007/s003970100161.

Chen, Y., Dong, K., Liu, Z., Xu, F., 2012. Double network hydrogel with high mechanical strength: performance, progress and future perspective. Sci. China Technol. Sci. 55, 2241–2254, http://dx.doi.org/10.1007/s11431-012-4857-y.

Gaharwar, A.K., Dammu, S.A., Canter, J.M., Wu, C.-J., Schmid, G., 2011. Highly extensible, tough, and elastomeric nanocomposite hydrogels from poly(ethylene glycol) and hydroxyapatite nanoparticles. Biomacromolecules 12, 1641–1650, http://dx.doi.org/10.1021/bm200027z.

Gong, J.P., 2010. Why are double network hydrogels so tough?. Soft Matter 6, 2583, http://dx.doi.org/10.1039/b924290b.

Gong, J.P., Katsuyama, Y., Kurokawa, T., Osada, Y., 2003. Double-network hydrogels with extremely high mechanical strength. Adv. Mater. 15, 1155–1158, http://dx.doi.org/10.1002/adma.200304907.

Gulsen, D., Chauhan, A., 2006. Effect of water content on transparency, swelling, lidocaine diffusion in p-HEMA gels. J. Memb. Sci. 269, 35–48, http://dx.doi.org/10.1016/j.memsci.2005.06.024.

Holloway, J.L., Spiller, K.L., Lowman, A.M., Palmese, G.R., 2011. Analysis of the in vitro swelling behavior of poly(vinyl alcohol) hydrogels in osmotic pressure solution for soft tissue replacement. Acta Biomater. 7, 2477–2482, http://dx.doi.org/10.1016/j.actbio.2011.02.016.

Jaramillo-Botero, A., Blanco, M., Li, Y., McGuinness, G., Goddard, W. a, 2010. First-principles based approaches to nano-mechanical and biomimetic characterization of polymer-based hydrogel networks for cartilage scaffold-supported therapies. J. Comput. Theor. Nanosci. 7, 1238–1256, http://dx.doi.org/10.1166/jctn.2010.1477.

Kong, H.J., Wong, E., Mooney, D.J., 2003. Independent control of rigidity and toughness of polymeric hydrogels. Macromolecules 36, 4582–4588, http://dx.doi.org/10.1021/ma034137w.

Kubinová, S., Horák, D., Hejčl, A., Plichta, Z., Kotek, J., Syková, E., 2011. Highly superporous cholesterol-modified poly(2-hydroxyethyl methacrylate) scaffolds for spinal cord injury repair. J. Biomed. Mater. Res. A 99, 618–629, http://dx.doi.org/10.1002/jbm.a.33221.

Livne, a, Cohen, G., Fineberg, J., 2005. Universality and hysteretic dynamics in rapid fracture. Phys. Rev. Lett. 94, 224301, http://dx.doi.org/10.1103/PhysRevLett.94.224301.

Maki, D.G., Tambyah, P.A., 2001. Engineering out the risk for infection with urinary catheters. Emerg. Infect. Dis. 7, 342–347.

Murakami, T., Higaki, H., Sawae, Y., Ohtsuki, N., Moriyama, S., Nakanishi, Y., 1998. Adaptive multimode lubrication in natural synovial joints and artificial joints. Proc. Inst. Mech. Eng. Part H J. Eng. Med. 212, 23–35, http://dx.doi.org/10.1243/0954411981533791.

Na, Y.-H., Kurokawa, T., Katsuyama, Y., Tsukeshiba, H., Gong, J.P., Osada, Y., Okabe, S., Karino, T., Shibayama, M., 2004. Structural characteristics of double network gels with extremely high mechanical strength. Macromolecules 37, 5370–5374, http://dx.doi.org/10.1021/ma049506i.

Naficy, S., Brown, H.R., Razal, J.M., Spinks, G.M., Whitten, P.G., 2011. Progress toward robust polymer hydrogels. Aust. J. Chem. 64, 1007, http://dx.doi.org/10.1071/CH11156.

Nakamura, 1976. Effects of various salts on the mechanical properties of homogeneous Poly(2-hydroxyethyl methacrylate) hydrogels. Polym. J.

Rongen, J.J., van Tienen, T.G., van Bochove, B., Grijpma, D.W., Buma, P., 2014. Biomaterials in search of a meniscus substitute. Biomaterials 35, 3527–3540, http://dx.doi.org/10.1016/j.biomaterials.2014.01.017.

Sachlos, E., Czernuszka, J.T., 2003. Making tissue engineering scaffolds work. Review: the application of solid freeform fabrication technology to the production of tissue engineering scaffolds. Eur. Cells Mater. 5, 29–39 discussion 39–40.

Šefca, L., Přádný, M., Vacík, J., Michálek, B., Povýšil, C., Vítková, I., Halaška, M., Šimon, V., 2002. Development of hydrogel implants for urinary incontinence treatment. Biomaterials 23, 3711–3715.

Spiller, K.L., Maher, S. a, Lowman, A.M., 2011. Hydrogels for the repair of articular cartilage defects. Tissue Eng. Part B Rev. 17, 281–299, http://dx.doi.org/10.1089/ten.TEB.2011.0077.

Sun, J.-Y., Zhao, X., Illeperuma, W.R.K., Chaudhuri, O., Oh, K.H., Mooney, D.J., Vlassak, J.J., Suo, Z., 2012. Highly stretchable and tough hydrogels. Nature 489, 133–136, http://dx.doi.org/10.1038/nature11409.

Tanaka, Y., 2007. A local damage model for anomalous high toughness of double-network gels. Europhys. Lett. 78, 56005, http://dx.doi.org/10.1209/0295-5075/78/56005.

Tanaka, Y., Fukao, K., Miyamoto, Y., 2000. Fracture energy of gels. Eur. Phys. J. E 401, 395–401.

Wang, Q., Hou, R., Cheng, Y., Fu, J., 2012. Super-tough double-network hydrogels reinforced by covalently compositing with silica-nanoparticles. Soft Matter 8, 6048, http://dx.doi.org/10.1039/c2sm07233e.

Webber, R.E., Creton, C., Polyme, L.D.P., Vauquelin, R., Brown, H.R., 2007. Large strain hysteresis and mullins effect of tough double-network hydrogels. Macromolecules 40, 2919–2927.

Ye, L., Tang, Y., Qiu, D., 2014. Enhance the mechanical performance of polyacrylamide hydrogel by aluminium-modified colloidal silica. Colloids Surf. A Physicochem. Eng. Asp. 447, 103–110, http://dx.doi.org/10.1016/j.colsurfa.2014.01.072.

Yin, H., Akasaki, T., Lin Sun, T., Nakajima, T., Kurokawa, T., Nonoyama, T., Taira, T., Saruwatari, Y., Ping Gong, J., 2013. Double network hydrogels from polyzwitterions: high mechanical strength and excellent anti-biofouling properties. J. Mater. Chem. B 1, 3685, http://dx.doi.org/10.1039/c3tb20324g.